Journal of Molecular Catalysis B: Enzymatic 62 (2010) 54–58

Contents lists available at ScienceDirect

Journal of Molecular Catalysis B: Enzymatic

journal homepage: www.elsevier.com/locate/molcatb

Evaluation of diatomaceous earth as a support for sol–gel immobilized lipase for transesterification

Sarah M. Meunier, Raymond L. Legge*

Department of Chemical Engineering, University of Waterloo, 200 University Avenue West, Waterloo, Ontario, Canada N2L 3G1

ARTICLE INFO

Article history:
Received 10 July 2009
Received in revised form 1 September 2009
Accepted 1 September 2009
Available online 11 September 2009

Keywords:
Enzyme immobilization
Sol–gel entrapment
Celite®
Transesterification
Lipase

ABSTRACT

Enzymatic production of biodiesel by triglyceride transesterification is a promising alternative to chemically catalyzed biodiesel production despite the challenges involved with using enzymes. Celite® supported lipase sol–gels were investigated as an option for solving some of the challenges associated with the use of enzymes for biodiesel production addressing such problems as activity, stability and reusability of the enzyme. Three types of Celite® were considered (R633, R632, and R647) and compared to unsupported lipase sol–gels. Various factors were considered with regard to comparing the support materials. They included surface morphology characterized using surface area analysis and scanning electron microscopy, physical properties including adhesion of the sol–gel to the Celite® and the protein loading on the Celite®, and finally enzymatic properties based on the conversion of methanol to methyl oleate and the enzymatic activity of lipase. All the sol–gels showed good conversion and initial lipase activity, and all the Celite® supports had similar sol–gel adhesion and protein loading. Sol–gel immobilized lipase supported on Celite® R632 had an average 6-h percent conversion of approximately 60%, and an average initial lipase activity comparable to that of the unsupported sol–gel formulation.

1. Introduction

Biodiesel is an alternative to fossil fuels that is becoming increasingly important due to environmental concerns, rising fossil fuel prices, demands for renewable fuel sources, and market requirements for agricultural surpluses [1]. Industrially, most biodiesel is produced using alkaline catalysts because this process is cost effective and efficient; however, it is energy intensive and requires significant downstream processing steps such as washing, separation and purification [2]. Alternatively, transesterification of triglycerides to produce biodiesel can be accomplished enzymatically using lipase. The enzymatic process consumes less energy, produces less waste and by-products, and involves milder operating conditions [3–6].

Industrially, enzymatic biodiesel production possesses several challenges including a slow reaction rate, the risk of enzyme inactivation by the alcohol substrate and glycerol by-product, and the high cost of enzymes [1]. By immobilizing enzymes, their reusability can be improved thereby reducing their associated costs, and simplifying downstream processing [3]. Further, lipase immobilized in sol–gel matrices has improved chemical and thermal stability and has higher activity compared to other immobilization procedures [7,8].

Sol–gel immobilized lipase can be supported on inert materials to improve the diffusion of substrates and products to and from the enzyme and thus improve the reaction rate [9–11]. Studies have shown that lipase supported on Celite 545® had greater activity, higher thermal stability, and improved reusability in comparison to lipase supported on Amberlite IRA-938® and free lipase [12–14]. Studies have also shown that sol–gel entrapped lipase immobilized on Celite 545® has improved activity and thermostability compared to lipase deposited directly on Celite 545® without using the sol–gel method [15,16].

Deactivation of lipase by methanol is a common challenge for the production of biodiesel via methanolysis. Although the stoichiometric ratio of oil to methanol is 1:3, studies have shown that enzyme deactivation can be significantly reduced by adding methanol in 3 steps of 1 mole ratio each [17–21]. Our own laboratory work using Novozym 435 supports this finding with an optimal methanol to triolein mole ratio of 0.5–1.5. As an alternative to stepwise methanolysis, one study shows that continuous addition of methanol was found to achieve the highest biodiesel conversion of 97% [22].

The presence of glycerol is also inhibitory to the enzymatic production of biodiesel [23]. Studies have shown that silica beds are successful for the adsorption of glycerol in biodiesel streams, but methanol is detrimental to this process [24,25]. Methanol desorbs glycerol from the silica [24], and adding methanol reduces the saturation capacity of the silica gel by half [25]. In addition, when silica gel was used to control the amount of water in the biodiesel system,

* Corresponding author. Tel.: +1 519 888 4567x36728; fax: +1 519 746 4979.
E-mail address: rllegge@engmail.uwaterloo.ca (R.L. Legge).

1381-1177/$ – see front matter © 2009 Elsevier B.V. All rights reserved.
doi:10.1016/j.molcatb.2009.09.002

excess silica reduced the biodiesel yield due to methanol adsorption [26].

The objective of this study was to better characterize lipase sol–gels supported on diatomaceous earth-based supports and to evaluate their efficacy in terms of the production of biodiesel via enzymatic transesterification. The surface morphology of the Celite® supported lipase sol–gels was characterized using surface area analysis and scanning electron microscopy. The physical properties investigated included the adhesion of sol–gel to the Celite® and the loading of protein on the Celite® sol–gel. Finally, the conversion and enzymatic activity of the hybrid materials were considered. For each property studied, three different types of Celite® were compared and, where applicable, the Celite® supported sol–gel was compared to unsupported sol–gel material. This information is valuable in evaluating an optimal support system for sol–gel immobilized lipase and for understanding the interaction between the support, sol–gel, and lipase.

2. Experimental

2.1. Materials

Celite® samples were a gift from World Minerals (Santa Barbara, CA). Lipase (NS44035) and Novozym 435 were gifts from Novozymes North America Inc. (Franklinton, NC). The biological source of NS44035 was not provided by the supplier; the commercial activity of NS44035 is 20,000 PLU/g. The biological source of Novozym 435 is *Candida antarctica* and its commercial activity is 10,000 PLU/g. Tetramethyl orthosilicate (TMOS), trimethoxypropylsilane (PTMS), triolein, and methyl heptadecanoate (HDA-ME) were obtained from Sigma–Aldrich Canada Ltd. (Oakville, ON). Sodium phosphate was obtained from Mallinckrodt Baker (Phillipsburg, NJ). Isopropyl alcohol was obtained from EMD Chemicals (Gibbstown, NJ). Hexane was obtained from Fisher Scientific Company (Ottawa, ON). The silica gel (6–12 mesh) was obtained from Eagle Chemical Co., Mobile, AL. Ultrapure water was produced using a Milli-Q water purification system from Millipore (Billerica, MA). All other chemicals were obtained from local suppliers and were of reagent grade.

2.2. Methods

2.2.1. Immobilization of lipase

To immobilize lipase on Celite®, 0.08 mol PTMS and 0.02 mol TMOS were hydrolyzed in the presence of 1 mol ultrapure water and 200 μL HCl (0.1 M). The mixture was sonicated in a water bath sonicator for 1 h. The precursor solution was then rotary evaporated in a heated water bath at 40 °C for 30 min to remove water and alcohol. A solution of lipase and phosphate buffer (50 mM, pH 7.0) with an approximate protein concentration of 4000 μg/mL was prepared, and 14 mL was added to the hydrolyzed precursor solution. Nine millilitres of the resultant mixture was combined with 6 g of the desired Celite® support, thoroughly mixed, and deposited in a Petri dish. The Petri dish was sealed and aged at 4 °C for 24 h. The gel was then dried unsealed at 4 °C until the drying rate was less than 1 mg/h. Once dry, the gel was removed from the Petri dish and washed to remove any protein not entrapped with the following wash sequence: twice with phosphate buffer (50 mM, pH 7.0, 5 mL per 3 mL sol–gel mixture), isopropyl alcohol (2.5 mL per 3 mL sol–gel mixture) and hexane (5 mL per 3 mL sol–gel mixture). Excess solvent was evaporated from the gel at room temperature overnight before the gels were stored in a sealed container at 4 °C.

Unsupported gels were prepared in a similar manner except that the evaporated precursor and enzyme mixture was deposited directly into a Petri dish for aging and drying; the dried sol–gel was crushed in a mortar following removal from the Petri dish, and the washing solutions were separated from the sol–gel by centrifugation at 4000 rpm for 10 min.

2.2.2. Surface area analysis

The nitrogen physisorption experiments were carried out in a Micrometrics Gemini 2375 surface area analyzer (Micrometrics Instrument Corporation, Norcross, GA). The samples were degassed at 120 °C for 15 h under nitrogen flow prior to each measurement. The Celite® R647 samples were degassed for an additional 3 h at 300 °C. StarDriver software was used to fit the adsorption curve and evaluate the BET surface area.

2.2.3. Scanning electron microscopy

The surface morphology of the gels was evaluated using a Hitachi S570 scanning electron microscope (Hitachi High-Technologies, Berkshire, England). The samples were coated with gold prior to analysis. An electron beam energy of 15 kV was used for analysis. Sol–gel clusters were identified visually from the SEM images, and the percent coverage of sol–gel on the surface of the Celite® particles was determined. For this analysis, 45 random images of each type of Celite® were collected and the percent coverage was determined for each image.

2.2.4. Protein determination

The total protein content of the gels was determined from the protein content of the enzyme solution loaded into the sol–gels and the protein content in the two buffer washes. The amount of protein was quantified using a Varian HPLC system (Varian Inc., Mississauga, ON) equipped with an Agilent Zorbax Bio Series GF-250 column (Agilent Technologies, Mississauga, ON) and calibrated using a BCA protein assay kit (Pierce Biotechnology Inc., Rockford, IL). The mobile phase for the HPLC analysis was 200 mM phosphate buffer (pH 7.0), and detection at an absorbance wavelength of 280 nm.

2.2.5. Enzymatic lipid transesterification

The enzymatic activity of the Celite® supported lipase sol–gels was determined by GC–MS analysis. The reactions were carried out at 40 °C with agitation for 6 h. The reaction vial consisted initially of approximately 1 g of the supported lipase sol–gel, 4 mmol of triolein, and 4 mmol of methanol. At 1 h intervals a 10 μL sample was removed from the reaction vial and diluted in 990 μL hexane and 100 μL of the internal standard, HDA-ME. The formation of methyl oleate, the reaction product, was followed using a Varian GC–MS system (CP-3800 gas chromatograph, Saturn 2000 mass spectrometer/mass spectrometer) equipped with a CP-Wax 52 CB fused silica column (CP8513, Varian Inc., Mississauga, ON). One microlitre sample of the diluted reaction mixture was injected into the GC at an injector temperature of 250 °C and a split ratio of 50. Helium was used as the carrier gas with a column flow of 1 mL/min. The GC oven temperature was initially set to 170 °C for 10 min, ramped at 10 °C/min to 250 °C, and held at 250 °C for 2 min.

3. Results and discussion

3.1. Surface morphology

Comparison of the textural characteristics of the three types of Celite® considered for this study, R633, R632, and R647 will be found in Table 1. The three types of Celite® were chosen based on their particle sizes and pore diameters. Surface area analysis was completed for each of the supports with and without a lipase sol–gel coating. The coated R633 had a significant increase in surface area over the uncoated R633, but the other two supports, R632 and R647, had no significant change in surface area upon coating

Table 1
Particle size and pore diameter for each type of Celite® based on the manufacturer's specifications, and surface areas of Celite® without lipase sol–gel (support) and with lipase sol–gel (coated). The confidence limits indicated represent the 95% confidence interval of the mean based on $n \geq 6$.

Celite	Particle size (μm)	Pore diameter (μm)	Support surface area (m^2/g)	Coated surface area (m^2/g)
R633	300–600	6.5	0.90 ± 0.12	1.37 ± 0.33
R632	600–1400	7	1.52 ± 0.17	1.49 ± 0.23
R647	600–1400	0.07	58.92 ± 0.77	64.39 ± 4.50

(Table 1). With R633, some sol–gel formation occurred between particles promoting particle agglomeration which could increase the surface area. In addition, the presence of sol–gel clusters on the Celite® confirmed that cohesive forces were perhaps stronger than the adhesive forces during sol–gel formation (Fig. 1). Sol–gel clusters were visible for all three types of Celite® (Fig. 1).

As seen in Fig. 2, R647 has significantly less percent sol–gel on the surface of the Celite® in comparison with R633 and R632. This indicates that the lipase sol–gel did not adhere as well to the Celite® R647 support. Celite® R647 has a much larger surface area (Table 1) than R633 and R632 which may favour sol–gel cohesion over adhesion to the Celite® surface.

3.2. Physical properties

Both the Celite® R633 and R632 have a comparable number of sol–gel clusters and average cluster size based on the 45 images recorded for each sample; however, Celite® R647 had very few clusters (Table 2). There is no significant difference between the levels of sol–gel adhesion on any of the support materials (Fig. 3). For R647, although the same mass of sol–gel is immobilized on the support (Fig. 3), the surface coverage is significantly lower (Fig. 2). This would suggest that the R633 and R632 favour adhesion of sol–gel as a thinner layer on the surface rather than cohesion of thicker sol–gel clusters as with R647.

Table 2
Quantification of the sol–gel clusters for each of the Celite® samples. 45 images for each type of Celite® were used for this determination.

	R633	R632	R647
Surface area imaged (μm^2)	477,000	477,000	477,000
Number of sol–gel clusters	38	48	2
Average cluster size (μm^2)	1,270	1,230	3,670
95% confidence interval for cluster size	540	480	6,130

Fig. 4 shows the loading of protein as calculated based on HPLC analysis. The unsupported sol–gel has a high protein loading per gram of material (Fig. 4A) because there is no additional mass contributed by the Celite® as is the case for supported sol–gels. When

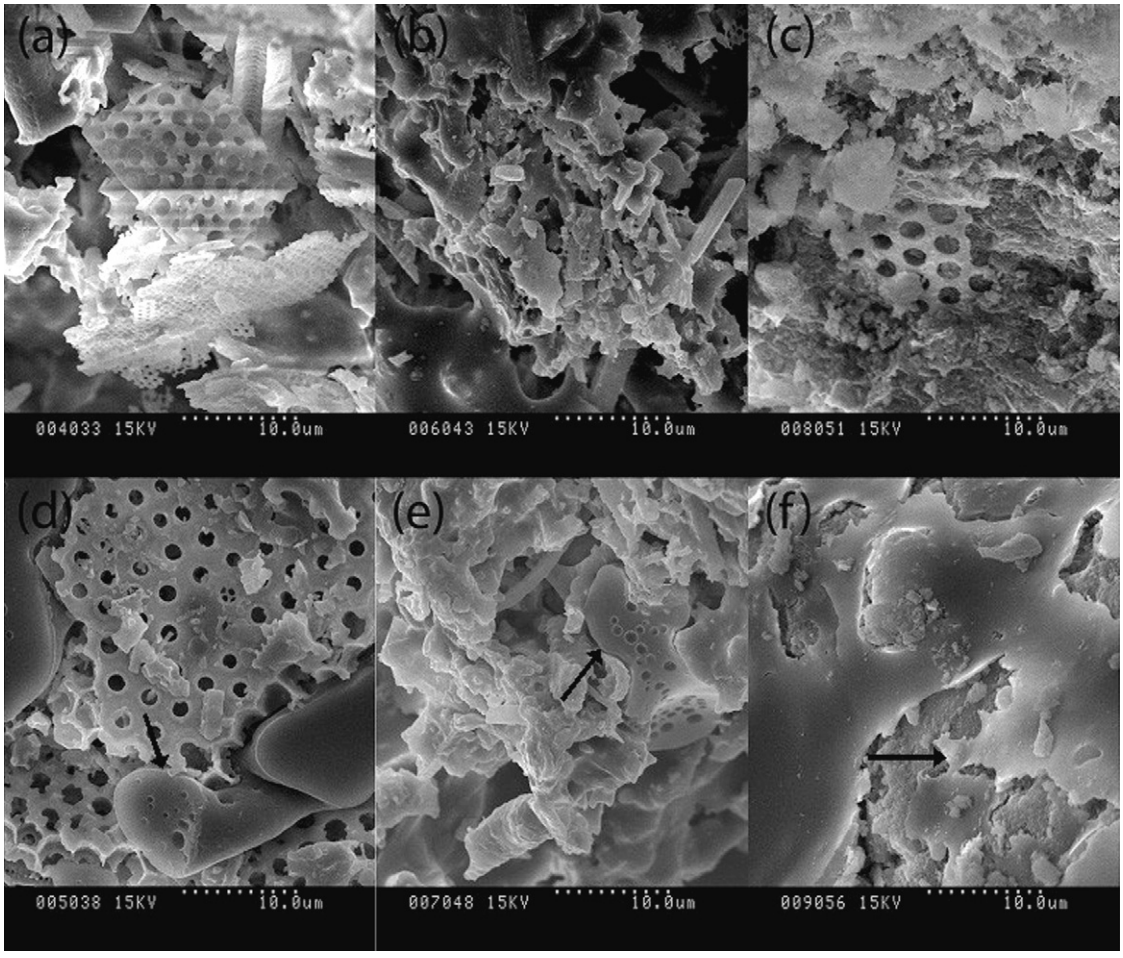

Fig. 1. SEM images at 3000× magnification of (a) uncoated Celite® R633, (b) uncoated Celite® R632, (c) uncoated Celite® R647, (d) Celite® R633 coated with lipase sol–gel, (e) Celite® R632 coated with lipase sol–gel, and (f) Celite® R647 coated with lipase sol–gel. Arrows identify some sol–gel clusters on the surface of the Celite®.

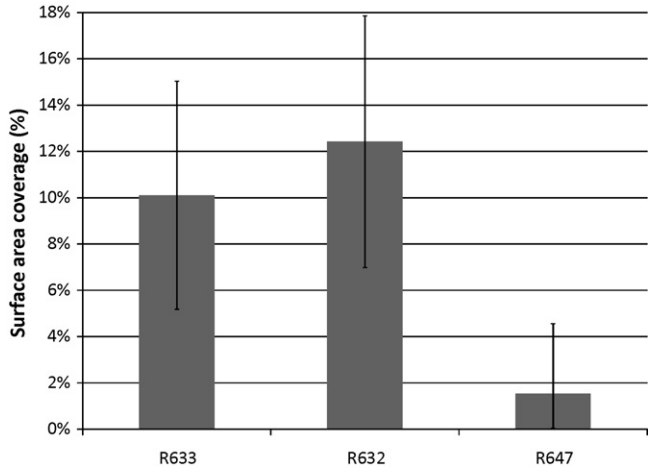

Fig. 2. Percent sol–gel coverage on the surface of Celite® as determined by SEM image analysis. The error bars represent the 95% confidence intervals of the sample mean based on $n = 45$.

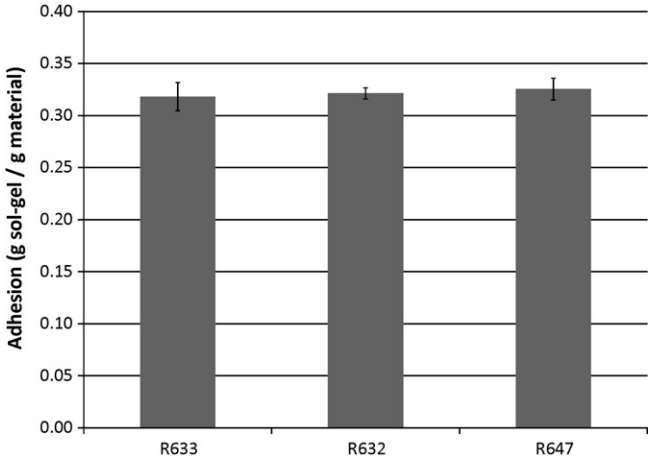

Fig. 3. Adhesion of sol–gel on the support for each type of Celite® considered. The error bars represent the 95% confidence intervals of the sample mean based on $n = 3$.

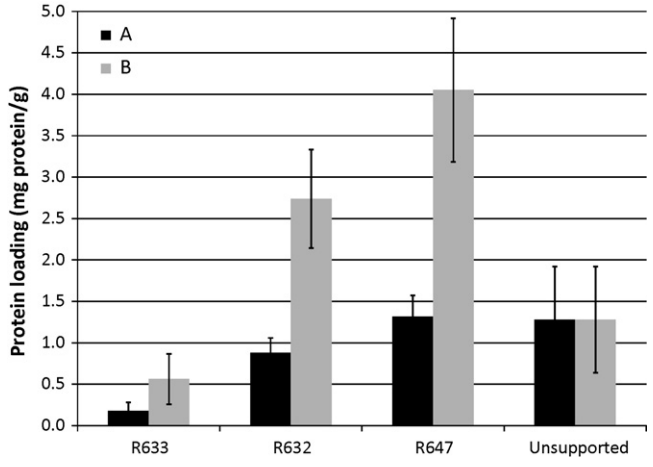

Fig. 4. Loading of protein per gram for each support: (A) the amount of protein per gram of material, and (B) the amount of protein per gram of sol–gel. The error bars represent the 95% confidence interval of the sample mean based on $n = 3$.

Table 3
Effect of the presence of silica gel and Celite® on methyl oleate production with Novozym 435 and unsupported sol–gel containing lipase.

Enzyme	Silica	Effect on methyl oleate production
50 mg Novozym 435	1 g silica gel	Reduction
200 mg unsupported sol–gel	1 g silica gel	Reduction
200 mg unsupported sol–gel	1 g Celite® R632	Elimination

the loading is considered on the basis of sol–gel only (Fig. 4B), the unsupported formulation is significantly lower than the Celite® R632 and R647 formulations. For both the material basis and sol–gel basis (Fig. 4A and B), R633 has significantly lower protein loading than R632 and R647. Based on the manufacturer's specifications for the Celite®, R633 has a much higher water adsorption capacity than R632 and R647 (R633 240%, R632 84%, and R647 163%). R633 may preferentially absorb the lipase-buffer solution from the sol–gel mixture, whereas the other types of Celite® absorb less water which may promote gelation of the lipase in the sol–gel polymer matrix. In the latter case the lipase would not be washed off the support as in the former case resulting in more protein immobilized on the R632 and R647 supports.

3.3. Enzymatic properties

Initial studies were performed to determine the effect of silica and Celite® on the enzymatic activity of the sol–gel. Adding 1 g of silica gel to either the 50 mg Novozym 435 or 200 mg sol–gel reaction systems reduced the amount of methyl oleate produced after 6 h (Table 3). Further, adding 1 g of Celite® R632 to the 200 mg sol–gel system caused no methyl oleate to be produced in 6 h. Therefore, any improved activity in the supported sol–gel appears to be due to the Celite® sol–gel complex rather than the adsorption of glycerol or water due to the presence of silica.

Fig. 5 shows the percent conversion of methanol to methyl oleate per gram of material based on a 6-h reaction period. R632, R647, and the unsupported sol–gels all show a higher conversion than R633. Since R633 has a lower protein loading than the other gels, a lower conversion per mass is expected. Fig. 6 shows that Celite® R633 exhibits a high initial lipase activity; however, its low protein loading and low conversion make it a poor support material for transesterification.

Fig. 6 shows that the initial lipase activity of the Celite® R647 is significantly lower than that of both R633 and R632. This would

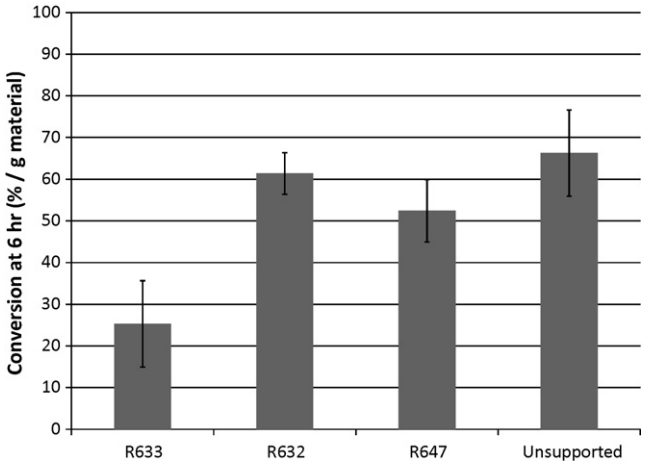

Fig. 5. Percent methanol conversion per gram of material after 6 h for each sol–gel formulation. The error bars represent the 95% confidence interval of the sample mean based on $n = 9$.

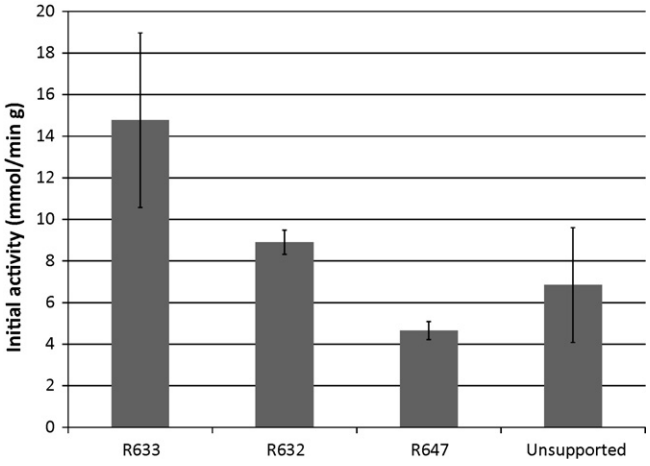

Fig. 6. Initial lipase activity for each sol–gel formulation measured by the initial amount of methyl oleate produced per minute per gram of protein. The error bars represent the 95% confidence interval of the sample mean based on $n = 9$.

indicate that the R633 and R632 supports provide a favourable environment for the immobilization of active lipase in comparison to R647. The high percent surface coverage (Fig. 2) on R632 while maintaining comparable sol–gel adhesion (Fig. 3) indicates that thinner layers of sol–gel are formed on the surface of this support, therefore the high lipase activity for the R632 lipase sol–gel may be due to improved internal mass transfer.

4. Conclusion

Lipase immobilized sol–gels supported on diatomaceous earth are promising for biodiesel production. All three Celite® supports considered (R633, R632, and R647) as well as the unsupported sol–gel exhibited lipase activity and showed conversion ranges from approximately 25% to 65% in 6 h. Similar sol–gel adhesion loadings were measured for each of the support materials. Based on the three support materials considered, Celite® R632 exhibited good initial activity and achieved an average conversion of approximately 60% per gram of material after 6 h of reaction. The high surface area coverage of the sol–gel on R632 indicates a thinner coating that would lead to improved internal mass transfer. Thus, comparing the three supports, Celite® R633, R632, and R647, and unsupported lipase sol–gel, Celite® R632 could be considered a promising support for lipase immobilized sol–gels to produce biodiesel via enzymatic transesterification.

Acknowledgements

This work was supported by the Natural Sciences and Engineering Research Council (NSERC) in the form of a Discovery grant to R.L.L. and an NSERC Postgraduate Scholarship to S.M.M. We thank Novozymes North America for supplying samples of the lipase formulation and World Minerals for supplying samples of the Celite® support materials.

References

[1] A. Robles-Medina, P.A. González-Moreno, L. Esteban-Cerdán, E. Molina-Grima, Biotechnol. Adv. (2009), doi:10.1016/j.biotechadv.2008.10.008.
[2] S.V. Ranganathan, S.L. Narasimhan, K. Muthukumar, Bioresour. Technol. 99 (2008) 3975–3981.
[3] C.C. Akoh, S.-W. Chang, G.-C. Lee, J.-F. Shaw, J. Agric. Food Chem. 55 (2007) 8995–9005.
[4] H. Fukuda, A. Kondo, H. Noda, J. Biosci. Bioeng. 92 (2001) 405–416.
[5] J.M. Marchetti, V.U. Miguel, A.F. Errazu, Renew. Sustain. Energ. Rev. 11 (2007) 1300–1311.
[6] P.T. Vasudevan, M. Briggs, J. Ind. Microbiol. Biotechnol. (2008) 1–10.
[7] M.T. Reetz, A. Zonta, J. Simpelkamp, Biotechnol. Bioeng. 49 (1996) 527–534.
[8] M.T. Reetz, Adv. Mater. 9 (1997) 943–954.
[9] T. Branyik, G. Kuncova, J. Paca, Appl. Microbiol. Biotechnol. 54 (2000) 168–172.
[10] O. Orcaire, P. Buisson, A.C. Pierre, J. Mol. Catal. B: Enzym. 42 (2006) 106–113.
[11] R.P. Pogorilyi, E.Y. Siletskaya, V.P. Goncharik, L.I. Kozhara, Y.L. Zub, Russ. J. Appl. Chem. 80 (2007) 330–334.
[12] A. Sağiroğlu, Artif, Cells Blood Substit. Immobil. Biotechnol. 36 (2008) 138–149.
[13] A. Sağiroğlu, A. Telefoncu, Prep. Biochem. Biotechnol. 34 (2004) 169–178.
[14] A. Sağiroğlu, A. Kilinç, A. Telefoncu, Artif. Cells Blood Substit. Immobil. Biotechnol. 32 (2004) 625–636.
[15] K. Kawakami, S. Yoshida, J. Ferment. Bioeng. 82 (1996) 239–245.
[16] K. Kawakami, Biotechnol. Tech. 10 (1996) 491–494.
[17] Y. Shimada, Y. Watanabe, T. Samukawa, A. Sugihara, H. Noda, H. Fukuda, Y. Tominaga, JAOCS 76 (1999) 789–793.
[18] Y. Watanabe, Y. Shimada, A. Sugihara, H. Noda, H. Fukuda, Y. Tominaga, JAOCS 77 (2000) 355–360.
[19] Y. Watanabe, Y. Shimada, A. Sugihara, Y. Tominaga, JAOCS 78 (2001) 703–707.
[20] Y. Watanabe, Y. Shimada, A. Sugihara, Y. Tominaga, J. Mol. Catal. B: Enzym. 17 (2002) 151–155.
[21] Y. Xu, W. Du, J. Zeng, D. Liu, Biocatal. Biotransfor. 22 (2004) 45–48.
[22] K. Bélafi-Bakó, F. Kovács, L. Gubicza, J. Hancsók, Biocatal. Biotransfor. 20 (2002) 437–439.
[23] T. Samukawa, M. Kaieda, T. Matsumoto, K. Ban, A. Kondo, Y. Noda, H. Fukuda, J. Biosci. Bioeng. 90 (2000) 180–183.
[24] J.C. Yori, S.A. D'Ippolito, C.L. Pieck, C.R. Vera, Energ. Fuel 21 (2007) 347–353.
[25] V.A. Mazzieri, C.R. Vera, J.C. Yori, Energ. Fuel 22 (2008) 4281–4284.
[26] L. Wang, W. Du, D. Liu, L. Li, N. Dai, J. Mol. Catal. B: Enzym. 43 (2006) 29–32.